JOURNAL OF MATERIALS SCIENCE, 30 (1995) 3820–3826

The influence of temperature and grain size on substructure evolution in stainless steel 316L

M. JANEČEK, K. TANGRI
Department of Mechanical Engineering, University of Manitoba, Winnipeg, Manitoba R3T 2N2 Canada

The flow stress of polycrystals is controlled by the processes occurring in the grain interior as well as in the mantle, i.e. at the grain boundary and its immediate vicinity. The early stages of evolution of dislocation substructure in these two regions with strain in 316L stainless steel polycrystals have been studied at 293 K, 673 K and 1123 K representing the low temperature thermal, the intermediate temperature athermal and the high temperature thermal regimes respectively. Specimens with grain sizes of 4 and 12 μm were employed to determine the effect of grain size.

Transmission electron microscopy studies on deformed specimens show the different roles of grain boundary and grain interior in different temperature regimes. In the low temperature regime grain boundaries act as obstacles to moving dislocations and as such high density of dislocation is found in the grain boundary vicinity. In the intermediate temperature regime the dislocations which are easily spread into the grain interior rearrange to form cell walls. In the high temperature regime grain boundaries transform to the equilibrium state and do not contain any grain boundary dislocations, and the distribution of dislocations within grains is homogeneous at all strains. Significantly higher values of dislocation densities in the vicinity as well as in the grain interior were found in the finer grain size material in the whole strain region employed.

1. Introduction

Grain boundaries play an important role during the early stages of plastic deformation of polycrystalline materials. It is generally recognized that grain boundaries act as dislocation sources and barriers to dislocation motion at low temperatures and sinks for dislocations at high temperatures [1–3]. In the early stage of plastic deformation there is a significantly higher accumulation of dislocations in the immediate vicinity of grain boundaries [4, 5] as compared to the grain interior, which leads to the formation of the so-called mantle. Thus in the regime of small strains, a polycrystalline material may be regarded to be consisting of two phases: a hard phase (mantle zone) and a soft phase (grain interior). The evolution of the substructure in these two regions during plastic deformation is significant for further deformation behaviour at higher strains and as such for work-hardening behaviour of polycrystals. In this regard, investigating the roles of the grain boundaries and the grain interior during strain-induced substructure development constitutes a necessary step in the understanding of deformation behaviour.

316L stainless steel polycrystals deformed in a wide range of temperatures exhibit three temperature regimes where the flow stress and strain hardening characteristics as well as the evolution of the microstructure are different [6]. In the low and high temperature thermal regimes (regime I: 293–473 K and regime III: 923–1173 K) the yield stress as well as the flow stress decreases with increasing temperature, whereas in the intermediate temperature athermal regime (regime II: 473–923 K) the stress and work-hardening rate increases with increasing temperature in this alloy.

The objective of this paper is to study the distribution of dislocations near the grain boundaries and within the grains and the evolution of dislocation substructure in early stages of plastic deformation in three different temperature regimes with the aim of understanding the different roles of the grain boundaries at the onset of plastic flow. Grain size is another structural parameter which may influence the evolution of the substructure. Therefore its effects are also considered in this study.

2. Experimental procedure

The experiments were performed on a commercial 316L stainless steel with a nominal composition (in wt %) of 0.017 C, 16.7 Cr, 11.2 Ni, 1.46 Mn, 2.04 Mo, 0.50 Si, 0.70 N, 0.032 P, 0.001 S and the balance Fe. The material was cold rolled to a 1.1 mm thick sheet in several passes at room temperature (92% reduction). Tensile specimens with a gauge length of 20 mm and gauge width of 5 mm were machined from this sheet. These specimens were then recrystallized for 1 h at 1198 and 1423 K to obtain two grain sizes with the mean intercept length of 3.9 and 12.04 μm,

0022–2461

respectively (the nominal grain size of 4 and 12 μm is used as a definition of grain size throughout the paper).

Tensile tests were performed at a strain rate of $10^{-4}\ s^{-1}$ on an Instron universal testing machine with an on-line PDP-11 system for data acquisition at three temperatures: 293, 673 and 1123 K. Specimens were strained to six different strain levels: 0.2, 0.5, 1, 2, 4 and 6%. Immediately upon reaching the desired strain level the specimens were quickly unloaded and rapidly quenched with a jet of liquid nitrogen.

Specimens for optical metallography were prepared using standard techniques which are described elsewhere [7]. Thin foil preparation for transmission electron microscopy (TEM) is described in detail elsewhere [8].

From TEM micrographs three different dislocation densities were evaluated:

1. ρ_{EGBD} the density of extrinsic grain boundary dislocations, i.e. the dislocations in the grain boundary plane,
2. ρ_V: dislocation density in a zone 1 μm wide on each side of a grain boundary, i.e. the dislocation density in the immediate vicinity of a grain boundary (the width of this zone was chosen arbitrarily), and
3. ρ_{GI}: dislocation density in the rest of the grain, i.e. the dislocation density in the grain interior.

The method of the evaluation of dislocation density from TEM micrographs using the intercept method of Smith and Guttman [9] is described elsewhere [8].

3. Results

The variation of dislocation densities with temperature and with the grain size were evaluated for the following conditions: (i) the temperature dependence of dislocation densities, i.e. the plots ρ_V–ε, ρ_{GI}–ε, and ρ_{EGBD}–ε for three temperatures (293, 673 and 1123 K) for a 12 μm grain size specimen; and (ii) the grain size dependence of dislocation densities, i.e. the plots of ρ–ε for two grain sizes (4 and 12 μm) at the specimens deformed at 673 K. Plots of ρ–ε for the specimens deformed at room temperature are shown in our previous paper [8].

Fig. 1 shows the variation of dislocation density ρ_V with strain for three different temperatures and for 12 μm grain size material. It is seen that up to 0.5% of strain ρ_V is relatively insensitive to temperature. For higher strains ρ_V increases with strain and the rate of increase is much more pronounced for a specimen deformed at low temperature. For higher strain the curves tend to reach saturation. The same kind of dependence was found for the 4 μm grain size material (not shown here).

In Fig. 2 plots of ρ_V versus ε for two different grain sizes and $T = 673$ K are shown. Significantly higher values of ρ_V were found in the finer grain size specimen in the whole strain region employed. The same kind of dependence was found at room temperature also [8].

Fig. 3 shows dislocation density in the grain interior ρ_{GI} for three deformation temperatures employed. At

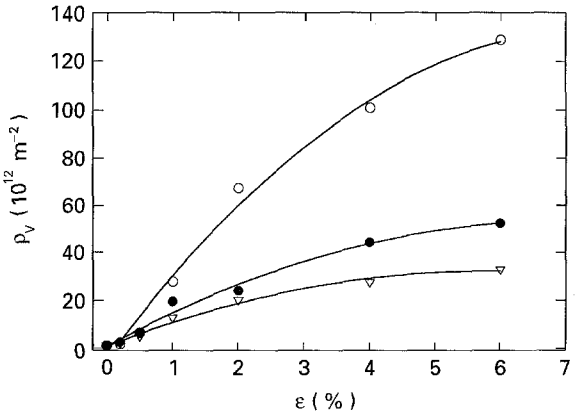

Figure 1 Variation in the dislocation density ρ_V with strain for three different temperatures: ○ 293 K; ● 673 K; ▽ 1123 K.

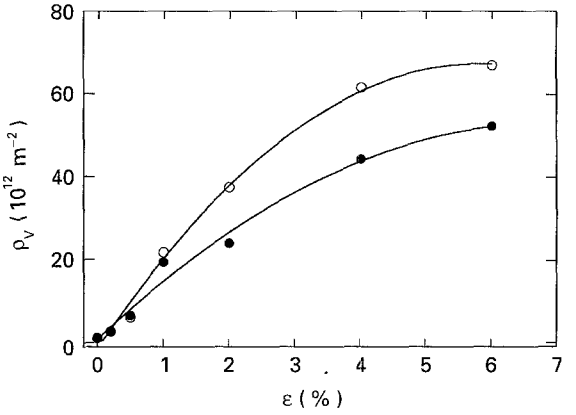

Figure 2 Strain dependence of the dislocation density ρ_V for two different grain sizes at 673 K: ○ 4 μm; ● 12 μm.

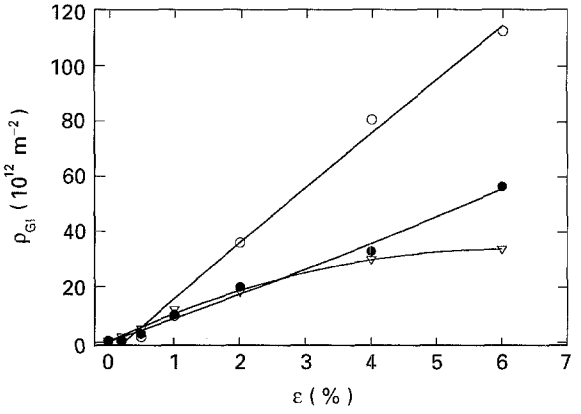

Figure 3 Evolution of the dislocation density in the grain interior ρ_{GI} for three deformation temperatures: ○ 293 K; ● 673 K; ▽ 1123 K.

room temperature ρ_{GI} increases almost linearly with ε. In the athermal temperature regime (represented by 673 K) ρ_{GI} also increases linearly with ε but at a considerably reduced rate as compared to that in the low temperature thermal regime (represented by 293 K). In the higher temperature thermal regime (represented by 1123 K) however, ρ_{GI} increases at the same rate as that in the athermal regime up to ≃4% strain where it reaches a saturation value.

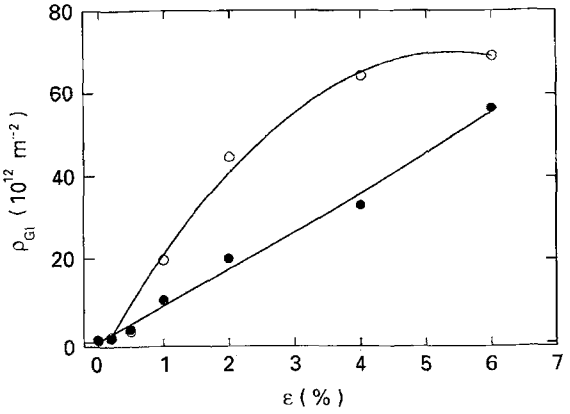

Figure 4 Strain dependence of the dislocation density ρ_{GI} for two different grain sizes at 673 K; ○ 4 μm; ● 12 μm.

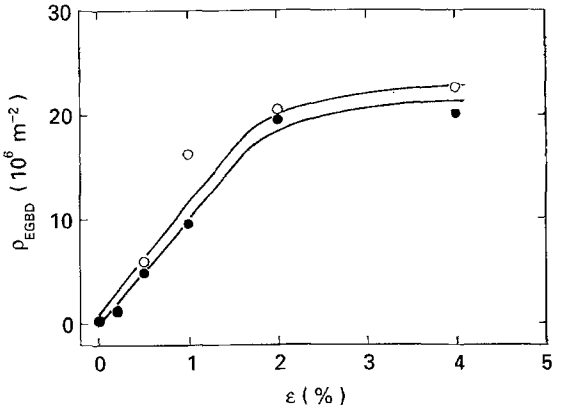

Figure 6 Variation in the density ρ_{EGBD} of extrinsic grain boundary dislocations with strain for two grain sizes: ○ 4 μm; ● 12 μm. ($T = 673$ K)

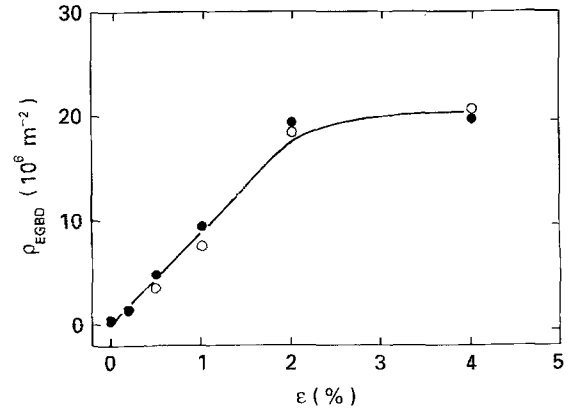

Figure 5 Variation in the density ρ_{EGBD} of extrinsic grain boundary dislocations with strain for two deformation temperatures; ○ 293 K; ● 673 K. ($d = 12$ μm)

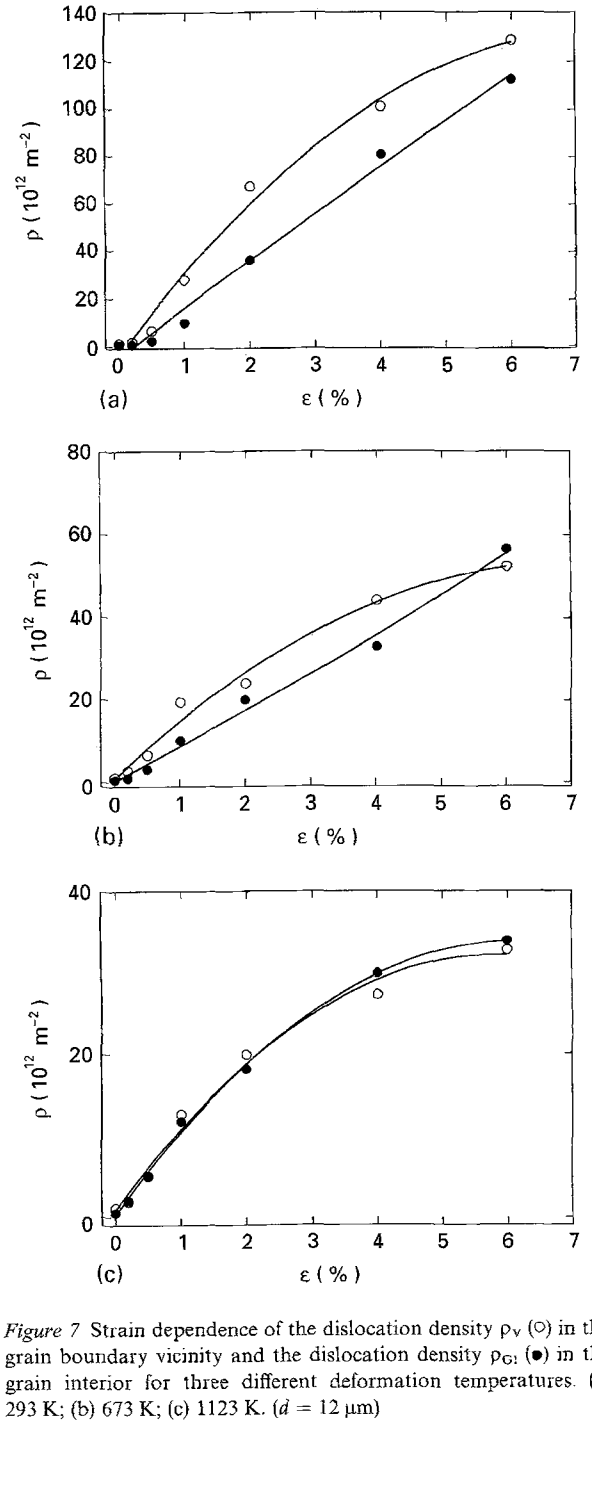

Figure 7 Strain dependence of the dislocation density ρ_V (○) in the grain boundary vicinity and the dislocation density ρ_{GI} (●) in the grain interior for three different deformation temperatures. (a) 293 K; (b) 673 K; (c) 1123 K. ($d = 12$ μm)

In Fig. 4 plots of density in the grain interior versus strain for two different grain sizes are shown. The effect of grain size on ρ_{GI} is seen to be similar to that on ρ_V, i.e. for a given strain ρ_{GI} decreases with increasing grain size. However, ρ_{GI} reaches a saturation value at about 5% strain in the 4 μm grain size material whereas it continues to increase linearly up to 6% strain in the 12 μm grain size material.

Figs 5 and 6 show the plots of density of EGBDs vs strain for two temperatures and two grain sizes, respectively. In all cases the density of extrinsic grain boundary dislocations (EDBDs) increases linearly up to 2% strain where it reaches a saturation value of about 22×10^6 m^{-1}. The influence of temperature as well as of grain size on ρ_{EGBD} is very weak. These observations are in good agreement with our previous work [8] and with the work of Varin and Tangri [10] who determined the saturation value of 27×10^6 m^{-1}. In the specimens deformed at 1123 K very few EGBDs were observed within the whole strain range employed. This annealing out of EGBDs on random grain boundaries at higher temperatures has been observed using *in situ* TEM technique by many authors [10–14].

Fig 7a–c shows the strain dependence of ρ_V and ρ_{GI} for three different temperatures. At room temperature (low temperature thermal regime, Fig. 7a)

TABLE Ia Strain dependence of the dislocation density ρ_v, ρ_{GI} and ρ_{EGBD} for three different temperatures ($d = 12$ μm)

ε(%)	$\rho_v(10^{12}\,m^{-2})$	$\rho_{GI}(10^{12}\,m^{-2})$	$\rho_{EGBD}(10^{6}\,m^{-1})$
$T = 293$ K			
0	1.1 ± 0.4	0.5 ± 0.2	0.4 ± 0.1
0.2	1.7 ± 0.6	0.6 ± 0.3	1.4 ± 0.5
0.5	6.6 ± 2.1	2.1 ± 1.4	3.5 ± 0.7
1	27.7 ± 0.7	9.6 ± 2.8	7.6 ± 1.9
2	67.4 ± 8.3	36.1 ± 4.6	18.7 ± 2.5
4	101.1 ± 16.9	80.8 ± 14.1	21.1 ± 3.6
6	128.9 ± 12.6	112.6 ± 11.5	full
$T = 673$ K			
0.2	2.6 ± 0.9	0.9 ± 0.5	1.3 ± 0.4
0.5	6.5 ± 3.4	3.1 ± 2.2	4.8 ± 0.7
1	19.4 ± 7.6	10.2 ± 3.5	9.5 ± 2.5
2	23.9 ± 7.3	20.0 ± 2.6	19.6 ± 3.2
4	44.3 ± 9.0	33.0 ± 7.3	20.1 ± 2.5
6	52.4 ± 9.4	56.6 ± 12.3	full
$T = 1123$ K			
0.2	1.9 ± 1.4	2.0 ± 0.9	0
0.5	5.0 ± 4.2	4.9 ± 1.9	0
1	12.6 ± 5.3	11.7 ± 4.2	0
2	19.9 ± 10.2	18.1 ± 8.7	0
4	27.4 ± 6.8	30.0 ± 9.4	0
6	32.8 ± 8.0	33.9 ± 6.4	0

TABLE Ib Strain dependence of the dislocation density ρ_v, ρ_{GI} and ρ_{EGBD} for two different temperatures ($d = 4$ μm)

ε(%)	$\rho_v(10^{12}\,m^{-2})$	$\rho_{GI}(10^{12}\,m^{-2})$	$\rho_{EGBD}(10^{6}\,m^{-1})$
$T = 293$ K			
0	1.1 ± 0.3	0.6 ± 0.3	0.4 ± 0.1
0.2	2.8 ± 0.6	1.1 ± 0.4	1.4 ± 1.0
0.5	9.8 ± 2.2	4.9 ± 1.1	4.9 ± 0.9
1	36.3 ± 3.6	13.3 ± 0.7	9.4 ± 3.7
2	88.8 ± 6.9	40.0 ± 2.4	20.0 ± 2.9
4	114.6 ± 11.0	90.2 ± 6.7	21.9 ± 3.0
6	139.4 ± 9.4	131.1 ± 8.4	full
$T = 673$ K			
0.2	2.7 ± 1.0	1.2 ± 0.8	1.2 ± 0.4
0.5	6.1 ± 3.1	2.7 ± 0.7	5.9 ± 1.3
1	21.7 ± 5.9	19.7 ± 7.2	16.2 ± 7.1
2	37.4 ± 7.5	44.7 ± 17.9	20.6 ± 2.9
4	61.7 ± 17.5	64.5 ± 16.4	22.6 ± 3.0
6	67.2 ± 15.0	69.3 ± 28.0	full

a significantly higher density of dislocations near the grain boundary as compared to the density in the interior of grains was observed ($\rho_V > \rho_{GI}$) for strains up to 6% [8]. In the athermal regime ($T = 673$ K, Fig. 7b) the difference between ρ_V and ρ_{GI} is much less pronounced, and at a strain of about 5.5% the density of dislocations within the grains becomes homogeneous, i.e. $\rho_V \approx \rho_{GI}$. In the high temperature thermal regime ($T = 1123$ K, Fig. 7c) the density of dislocations is very low and almost uniform from the very beginning of deformation.

The results of all measurements are summarized in Table I.

4. Discussion

The evolution of microstructure during straining at room temperature was described in our previous paper [8]. We will now concentrate on the description of structural changes during deformation in the athermal regime (673 K) and high temperature thermal regime (1123 K).

At the onset of straining in the athermal regime an increased dislocation density in the immediate vicinity of the grain boundaries was observed (Fig. 8a, b). The dislocations are either randomly distributed in this area, or form pile-ups. The crucial question which arises is whether these dislocation arrangements are pile-ups or emission profiles, in other words whether a grain boundary has acted as a sink and then an obstacle for a moving dislocation which was emitted by a source inside the grain [15], or some structural feature of the grain boundary (a kink or ledge) has acted as a source of dislocations which were then emitted into the grain [16] ?

For the interpretation of TEM micrographs one must distinguish between the "instantaneous" state and the "relaxed" state. The "instantaneous" state means the actual state of the microstructure of the bulk specimen and the "relaxed" state is the microstructure observed in the thin foil made from this bulk specimen. It is very probable that for intermediate temperatures of deformation the "instantaneous" microstructure differs from the "relaxed" one for the following reasons. Firstly, the quench, even when made by liquid nitrogen, is not sufficiently rapid to "freeze" the "instantaneous" structure. Secondly, the "relaxed" state is the state upon unloading and therefore all processes related to the relaxation of the "instantaneous" structure have to be considered. Thus, it is hard to imagine that in the "relaxed" state one may observe dislocations which were not pinned at the moment when the deformation was stopped ("instantaneous" state). On the other hand, the dislocation configurations in the form of a pile-up against the grain boundary are probably sufficiently pinned to resist all relaxation processes and remain unchanged during unloading, the quench and foil preparation. One may then conclude that the main part of dislocations which we observe on our TEM micrographs of specimens strained up to 1% are parts of dislocation loops emitted by a source inside the grain and piled up against a grain boundary. In a small grain size material, it is possible that dislocations generated at a grain boundary segment may travel across the grain to produce a pile-up.

As the deformation proceeds the secondary or multiple slip in the neighbouring grain or in the vicinity of the grain boundary is activated [17, 18] in order to accommodate the intragranular slip in the grain boundary region. The dislocations which are generated may easily travel into the grain interior and thus the dislocation density ρ_{GI} increases with increasing strain. Moreover, at intermediate temperatures cross-slip is facilitated by the temperature which leads to the rearrangement of dislocations into low-energy configuration such as cell walls or dislocation bands. The onset of the formation of cell structure is seen on the TEM micrographs (Fig. 8c, d). The results of our previous study [8] (Fig. 8) have shown that at room temperature cell formation is not observed because of the difficulty of cross-slip in this temperature regime.

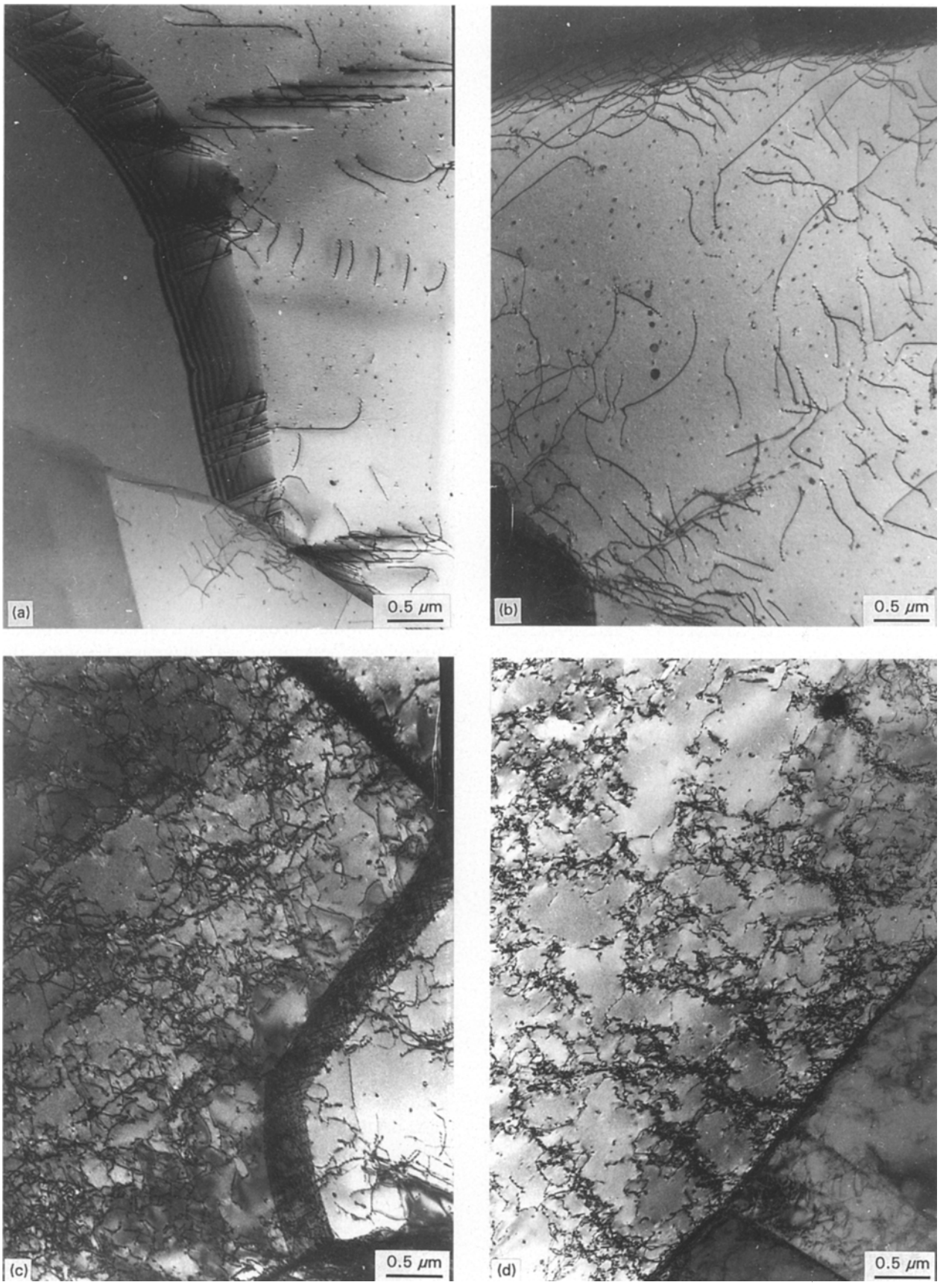

Figure 8 A series of TEM micrographs illustrating the evolution of the microstructure of the specimen deformed at $T = 673$ K. (a) $\varepsilon = 0.5\%$; (b) $\varepsilon = 1\%$; (c) $\varepsilon = 4\%$; (d) $\varepsilon = 6\%$.

In the high temperature regime ($T = 1123$ K), similar kinds of dislocation pile-ups near grain boundaries were observed at the onset of straining (Fig. 9a, b). With further straining, dislocations reaching the grain boundary during intragranular slip may easily glide or climb along the boundaries and participate in grain boundary sliding, and thus there is no need for continuous dislocation generation in order to accommodate the intragranular slip. As the mobility of dislocations is very high, they can easily cross-slip

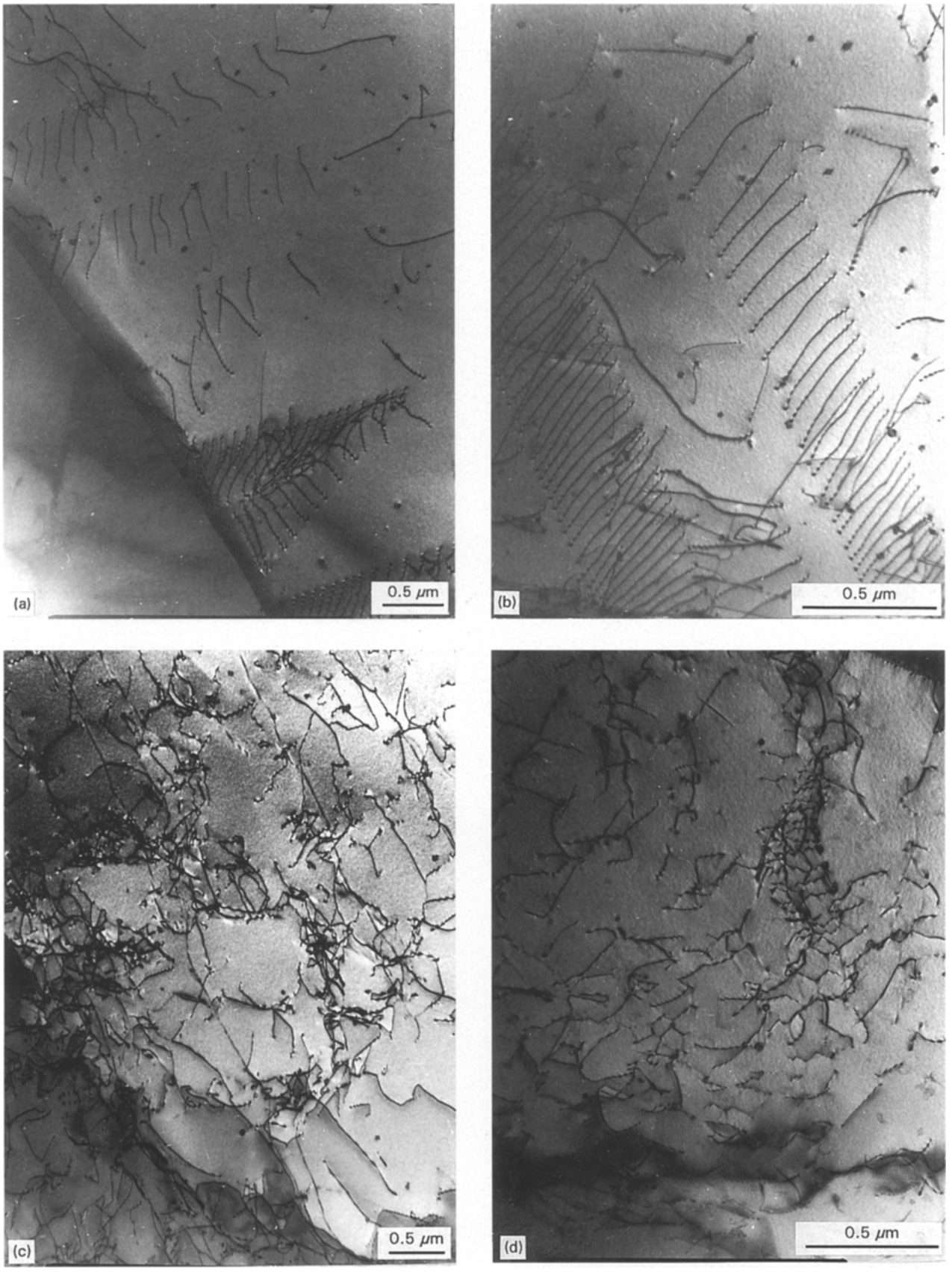

Figure 9 Transmission electron micrographs illustrating the microstructure evolution during the deformation at 1123 K. (a) $\varepsilon = 0.5\%$; (b) $\varepsilon = 1\%$; (c) $\varepsilon = 4\%$; (d) $\varepsilon = 6\%$.

as well as climb and therefore their density is relatively low and the distribution within grains rather homogeneous (Fig. 9c, d).

TEM observations show that the temperature of deformation has a significant effect on the appearance of dislocations in the grain boundary. At 673 K grain boundaries are full of EGBDs (Fig. 10a), whereas at high temperature (1123 K) the grain boundaries are almost free of EDBDs (Fig. 10b). This annihilation of EGBDs at high temperatures is associated with the migration of grain boundaries and leads to the changes in the structure of grain boundaries and their

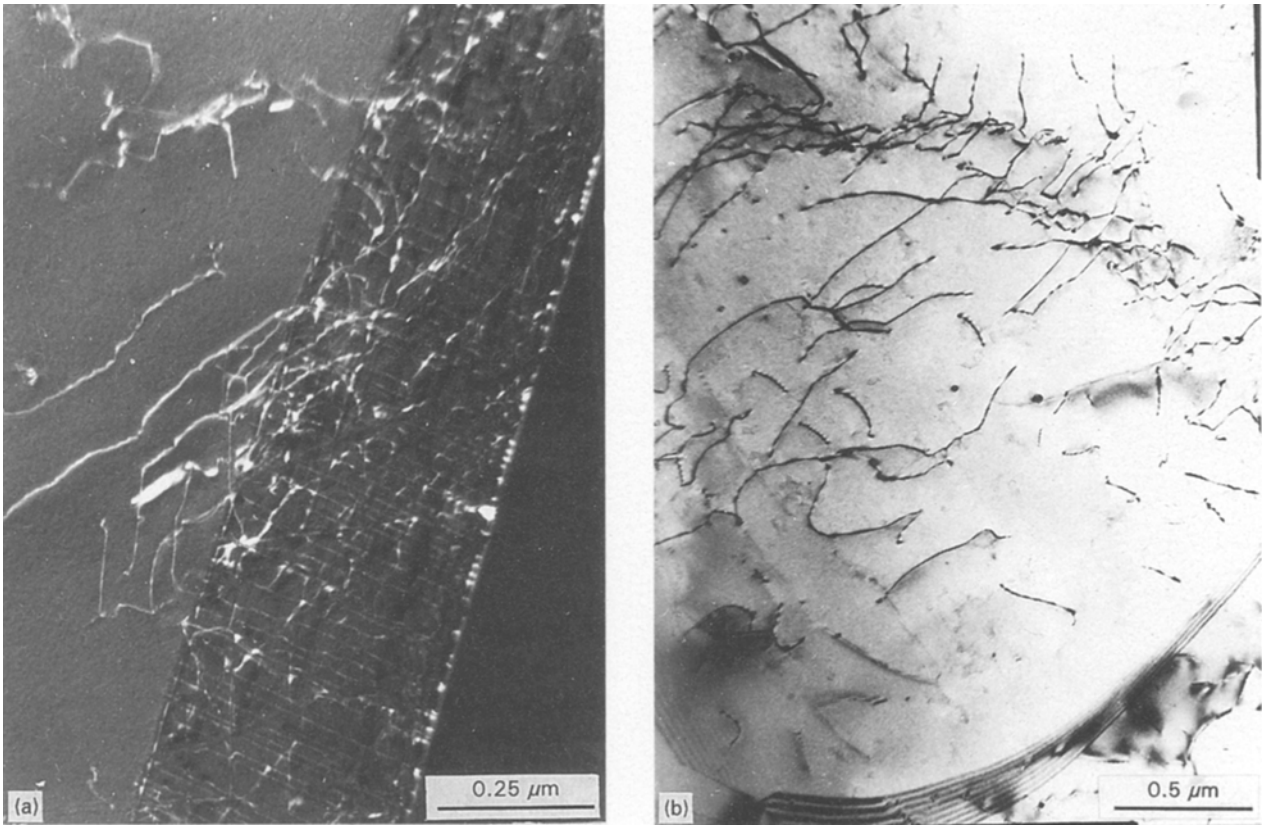

Figure 10 The dislocation structure in the grain boundary upon straining ($\varepsilon = 6\%$) at two different temperatures: (a) $T = 673$ K; (b) $T = 1123$ K.

transformation from non-equilibrium to equilibrium state as has been reported by Kurzydlowski *et al.* [4] and Sangal and Tangri [2].

5. Conclusions

1. The temperature of deformation has a significant effect on the substructure evolution in the grain boundary, its vicinity as well as in the grain interior.

2. In the low and medium temperature regimes grain boundaries act as barriers to dislocation motion whereas at high temperatures they act as sinks.

3. In the low and medium temperature region the grain boundaries are in non-equilibrium state, i.e. they include EGBDs. In the high temperature region grain boundaries are free of EGBDs, i.e. they are in the equilibrium state.

4. Significantly higher values of ρ_V and ρ_{GI} were found in the finer grain size material in the whole strain region employed.

5. The effect of grain size on the evolution of the density of EGBDs is very weak in the low and intermediate temperature regime.

Acknowledgements

This work was financially supported by the NSERCC. The technical assistance of Messrs D. Mardis and J. Van Dorp is appreciated.

References

1. T. MALIS and K. TANGRI, *Acta Metall.* **27** (1979) 25.
2. S. SANGAL and K. TANGRI, *Metall. Trans.* **20A** (1989) 479.
3. L. E. MURR, *ibid.* **A6** (1975) 505.
4. K. J. KURZYDLOWSKI, S. SANGAL and K. TANGRI, *ibid.* **20A** (1989) 471.
5. L. E. MURR and S. H. WANG, *Res. Mechanica* **4** (1982) 237.
6. B. P. KASHYAP, K. McTAGGART and K. TANGRI, *Phil. Mag.* **A57** (1988) 97.
7. F. C. BELL and D. E. SONON, *Metallography* **9** (1976) 91.
8. M. JANEČEK and K. TANGRI, *Mat. Sci. Engng* **A138** (1991) 237.
9. C. S. SMITH and L. GUTTMAN, *Trans. Metall. Soc. AIME* **197** (1953) 81.
10. R. VARIN and K. TANGRI, *Metall. Trans.* **A12** (1981) 1859.
11. Y. ISHIDA, T. HASEGAWA and F. NAGATA, *Trans. J. Inst. Metals* **9** (1968) 504.
12. P. H. PUMPHREY and H. GLEITER, *Phil. Mag.* **A30** (1974) 593.
13. W. LOJKOWSKI and K. GRABSKI, *Scripta Metall.* **13** (1979) 511.
14. T. JOHANNESSON and A. THOLEN, *Metal. Sci.* **6** (1972) 189.
15. R. Z. VALIEV, V. Y. GERTSMAN and O. KAIBYSHEV, *Phys. Stat. Sol.* **a97** (1986) 11.
16. L. E. MURR, *Mat. Sci. Engng* **51** (1981) 79.
17. T. LEFFERS, in "Deformation of polycrystals: Mechanisms and microstructures", edited by N. Hansen, A. Horsewell, T. Leffers and H. Lilhot (Roskilde: Risø National Laboratory, 1981) p. 55.
18. J. J. HAUSER and B. CHALMERS, *Acta Metall.* **9** (1961) 802.

Received 8 September 1994
and accepted 23 February 1995